

ION HOMEOSTASIS AND OSMOREGULATION IN *TAMARIX DIOICA* ROXB. EX ROTH THROUGH MODULATION OF STRUCTURAL AND FUNCTIONAL FEATURES

ZAHER UDDIN BABAR¹, IFTIKHAR AHMAD^{1*}, MANSOOR HAMEED²
AND MUHAMMAD SAJID AQEEL AHMAD²

¹Department of Botany, University of Sargodha, Sargodha 40100, Pakistan

²Department of Botany, University of Agriculture, Faisalabad 38040, Pakistan

*Corresponding author's email: iak8767@yahoo.com

Abstract

Salt indicator species inhabiting wild habitats could provide important information regarding salinity-tolerance mechanisms in plants. In this study, *Tamarix dioica* populations were collected from saline habitats all over the Punjab i.e., from Khabeki Lake, Uchali Lake, Kallar Kahar Lake, Katha Saghral, Lilla range, Kirrana hills, and Faisalabad. Their salinity tolerance potential was accessed based on growth, photosynthetic pigments, oxidative stress indicators, anti-oxidative enzyme activities, and anatomical attributes. Many populations of *Tamarix dioica* maintained chlorophyll contents at high salinities. Higher accumulation of proline, glycine betaine, free amino acids, soluble sugars, soluble proteins, and ascorbic acid contributed to growth maintenance under saline environments. An increase in the shoot potassium, calcium, and magnesium was consistent with a concurrent decrease in shoot sodium. Among the anatomical features, an increase in root epidermis thickness, cortex, endodermis, phloem, vascular bundle, metaxylem, pith, and sclerification was recorded intolerant populations. Similarly, stem epidermis, cortex, metaxylem, phloem, and vascular bundle areas increased under salt stress. All these features differentially enabled *T. dioica* populations to survive in highly saline environments.

Key words: Ion homeostasis, Osmoregulation, Anatomical modifications, Salinity tolerance, *Tamarix dioica*.

Abbreviations: 153R: Chak 153 RB; ASA: Ascorbic acid; Ca²⁺: Shoot calcium; Car: Carotenoids; CellRTh: Stem thickness; Chl a: Chlorophyll a; Chl b: Chlorophyll b; CortCA: Cortical cell area; CortTh: Cortical thickness; CRCA: Cortical region cell area; CRTh: Cortical region thickness; EndCA: Endodermal Cell area; EndoTh: Endodermal thickness; EPiCA: Epidermal cell area; EPiTh: Epidermal cell area; EpiTh: Epidermal thickness; FAA: Free amino acids; GB: Glycinebetaine; H₂O₂: Hydrogen peroxide; K⁺: shoot potassium; Khab: Khabike Lake; Kir: Kirrana Hills; lai: Leaf area index; Lill1: Lillah 1; Lill2: Lillah 2; Lpp: Leaves per plant; Mg²⁺: Shoot magnesium; MXCA: Metaxylem cell area; MXTh: Metaxylem cell area; MXTh: Metaxylem thickness; Na⁺: Shoot sodium; P111: Pull 111; Ph: Plant height; PhCA: Phloem cell area; PhTh: Pith cell area; PhTh: Phloem thickness; PhTh: Pith thickness; PithCA: Pith Cell area; PithTh: Piththickness; Pkh2: Peer Khara 2; Pkh1: Peer Khara 1; POD: Peroxidase; Pro: Proline; RR: Root radius; Rt: Root length; ScA: Sclerenchymatous cell area; ScTh: Sclerenchyma thickness; Sdw: Shoot dry weight; Sfw: Shoot fresh weight; SHA: Sahianwala A; SHB: Sahianwala B; SHC: Sahianwala C; SP: Soluble proteins; SS: Soluble sugars; Sug: Katha Saghral; Ucha: Uchali Lake; VBCA: Vascular bundle cell area; VBNo: Vascular bundle number; VBTh: Vascular bundle thickness; VBTh: Vascular bundle thickness

Introduction

Soil salinization is the driving factor for land degradation all over the world. Salt-induced soil degradation is increasing rapidly, mainly due to the excessive use of fertilizers, poor irrigation practices, and increasing dryness (Meena *et al.*, 2019). Worldwide, saline soils account for more than 831 Mha of the total world's area (Amini *et al.*, 2016), including 434 Mha of sodic and 397 Mha of saline soils (Anon., 2015). In Pakistan, salinity-affected areas are more than 7 Mha containing both saline and sodic soils (Anon., 2017). Therefore, targeting salt-tolerant plant species to rehabilitate these salt-affected soils is the basic necessity for the current era (Liang *et al.*, 2017). Identifying salt-tolerant plant species has a massive potential to rehabilitate these salt-affected soils (Glenn *et al.*, 2013).

Salt stress causes numerous effects on plant growth and development. These effects can be observed at cellular and whole plant levels due to physiological and molecular processes disturbance. For example, salt stress caused a higher accumulation of Na⁺ in the chloroplast, which ultimately resulted in chlorosis and disruption of plant tissues (Flowers *et al.*, 2015). Furthermore, such a high accumulation of cytosolic Na⁺ reduces the osmotic

potential of mesophyll cells in leaves, impairing the photosynthetic electron transport chain (Chaves *et al.*, 2009). Apart from this, higher production of reactive oxygen species further inhibits plant growth in saline soils (Flowers *et al.*, 2015). By contrast, salt-tolerant plant species efficiently quench reactive oxygen species (ROS) by up-regulation of antioxidant enzymes and maintaining ionic homeostasis in the cytosol (Guo *et al.*, 2021).

Halophytes counter salinity mainly by osmotic adjustments, exclusion, and homeostasis of Na⁺ to achieve tolerance by tissue-specific modifications (Kumari *et al.*, 2019). These salt-tolerant plants have achieved modifications in photosynthetic machinery over the course of evolution, which enable them to thrive under saline extremities without compromising growth and photosynthesis (Himabindu *et al.*, 2016). Major adaptations include structural and functional modifications to avoid Na⁺ and Cl⁻ accumulation at the cellular level (Joshi *et al.*, 2015). In addition, salt-tolerant plants exhibit many structural and functional changes in the ultrastructure of leaf chloroplast *i.e.*, having larger mesophyll cells in the broad lamina (Rozentsvet *et al.*, 2016). Furthermore, many obligate halophytes show improved water use efficiency, leading to an improved net CO₂ assimilation rate (Rabhi *et al.*, 2012).

Tamarix dioica Roxb. ex Roth is the most suitable species to combat land degradation in changing climatic conditions. This genus consists of halophytic shrubs and trees native to Southern Europe, North Africa, the Middle East, and South Asia (Gaskin & Schaal, 2002). Due to their fast growth, easy vegetative propagation, and acclimation capability to a wide range of contrasting environmental conditions, these plants are of particular interest (Daoyuan *et al.*, 2003). Most importantly, members of this genus show various protective mechanisms that ensure survival and growth in harsh environments (Jasiem *et al.*, 2019). One of the primary mechanisms includes the presence of salt glands on leaves, which play an important role in regulating ionic balance and regulating osmotic and turgor pressure under high salinity. It was hypothesized that different populations growing in hyper-saline habitats should have evolved different structural adaptations to assist ion homeostasis for enhanced salinity tolerance. Keeping in view, the current study was conducted to investigate the role of ion homeostasis and osmoregulation in the adaptability of *Tamarix dioica* Roxb. ex Roth to diversified environments through modulation of structural and functional features.

Materials and Methods

Site Selection and sampling: Eleven sites [Kirrana hills (31.97N, 72.70E), Katha Saghral (32.52N, 72.44E), Kallar Kahar 1 (32.79N, 72.69E), Kallar Kahar 2 (32.76N, 72.69E), Lilla 1 (32.58N, 72.73E), Lilla 2 (32.54N, 72.78E), 153 Rakh branch (31.59N, 73.30E), Sahianwala site B (31.63N, 73.24E), Sahianwala site C (31.67N, 73.21E), Khabbeki Lake (i), Uchali Lake (32.55N, 72.03E)] were selected from five ecological ecozones (salt marshes, waterlogged salinity, seasonal inundation, dry-land salinity, and saline desert) of Punjab during 2017-18. These sites were selected based on their ecological and edaphic characteristics, especially soil composition, salinity level, habitat, and vegetation type. Ten plants (replicates) were collected from each selected salt-affected ecozones. The plants were immediately placed in zipper bags and stored in the icebox for laboratory analysis.

Soil analysis: Soil samples (in three replicates) adhering to the rooting zone of each plant from all habitats up to 30 cm depth were taken to analyze the physicochemical characteristics. The well-mixed soil samples were extracted with vacuum and used to determine the pH and ECe using a pH/EC meter (Inolab, WTW series, UK). The protocol of Moodie *et al.*, (1959) was followed to determine soil texture. Sodium (Na^+), potassium (K^+), and calcium (Ca^{2+}) contents were measured from a soil saturation paste extract with a flame photometer (Jenway, PFP-7).

Analyses of biochemical characteristics

Ionic content of root and shoot: Dried shoot and root material (0.5 g) were digested with sulphuric acid and hydrogen peroxidase for the quantification of various ions viz., calcium, sodium, and potassium (Wolf, 1982) using a flame photometer (Jenway, PFP-7).

Organic osmolytes: Free amino acids were estimated following Hamilton & Van Slyke (1943). Total soluble sugars were evaluated by the method of Yemm & Willis (1954). Total soluble proteins were determined following Lowry *et al.*, (1951). Glycinebetaine was assessed by the procedure of Grieve & Grattan (1983), while proline was determined following Bates *et al.*, (1973).

Oxidative stress indicators: The procedure of Goliber (1989) was used for quantification of leaf peroxidase (POX). Hydrogen peroxide was determined by following Velikova *et al.*, (2000).

Leaf ascorbic acid: Leaf ascorbic acid was assessed by method of Mukherjee & Chaudhary (1983).

Anatomical characteristics: Anatomical characteristics were studied from permanent slides prepared by free hand sectioning. For the anatomical investigations, a piece (2 cm) was taken from the longest branch and from base of the thickest root of same plant. The samples were fixed in FAA solution (v/v formalin 10%, acetic acid 5%, ethyl alcohol 50% and refined water 35%) for 48 h. After that, the samples were shifted to another solution (v/v acetic acid 25%, and ethanol 75%) for long-term storage. The samples were dehydrated in graded series of ethanol following staining with standard double-stained using safranin and fast green. Photographs were taken with the help of a camera-equipped light microscope (Nikon 104, Japan) using an ocular micrometer, which was calibrated with a stage micrometer. For root anatomy, dermal tissue (epidermis, root hair), ground tissue (parenchyma, sclerenchyma) and vascular tissue (xylem, phloem) were measured. For stem anatomy, stem cross-sectional area, dermal tissue (epidermis, root hair), ground tissue (parenchyma, sclerenchyma), and vascular tissue (xylem, phloem) were measured.

Statistical analysis: The statistical package Minitab was used for calculation of least significant differences (LSD) following Steel *et al.*, (1997). Canonical Correspondence Analysis (CCA) triplot were constructed using Canoco for windows (v 4.0).

Results

Soil characteristics: The soil was collected from different saline habitats to determine pH, ECe, TDS, OM, APho, Na^+ , K^+ , Ca^{2+} , and Mg^{2+} . The CCA triplot for soil and sites showed the low influence of sodium, calcium, and magnesium with Sahianwala site B. Similarly, soil sodium showed weaker influence on Khabbeki, Kallar Kahar1, and Lilla1 sites along with low potassium and calcium as compared to other sites. Kallar Kahar site 3 also showed low influence of sodium and high with potassium and calcium, as they were plotted away from the magnesium. These sites contained low sodium, electrical conductivity, and total dissolved salts. On the other hand, all other sites i.e., Sahianwala site C, Kirrana, Katha Saghral, Peer Khara, Uchali, 153 RB, Kirrana 2, Peer Khara1, Lilla 2, Kirrana 1, Peer Khara 2 and Pull 111

did not show much variation in soil sodium, potassium, calcium as well as magnesium. Peer Khara and 153 RB contained maximum electrical conductivity. Lilla1, Peer Khara and 153 RB contained maximum total dissolved salts. Available phosphorus did not cause any significant variation among sites. Organic matter was equally distributed among the sites except in Kallar Kahar 2, Katha Saghral, and Khabbeki Lake that contained lower organic matter (Fig. 1).

Shoot ionic contents: Shoot Na^+ was the highest in plants collected from Sahianwala C site and lowest in plants inhabiting Khabbeki Lake. Shoot K^+ was the maximum in Khabbeki Lake population and the minimum in plants belonging to Katha Saghral site. The Mg^{2+} concentration

was the highest in plants collected from 153 RB and Peer Khara 2 sites. The lowest concentration was found in Kirrana hills and Pull 111 populations. Shoot Ca^{2+} value was the highest in plants inhabiting Peer Khara and the lowest in those collected from Lilla 2 and Katha Saghral sites (Table 1).

Photosynthetic pigments: The concentration of *Chl a* was the highest in plants inhabiting Lilla1 and lowest in plants collected from Khabbeki Lake and Peer Khara 2. The *Chl. b* was the highest in plants of Lilla1 population and the lowest in plants inhabiting Khabbeki Lake, Sahianwala C site, and Katha Saghral sites. Carotenoid contents were the maximum in Lilla1 population and the lowest in plants collected from Khabbeki Lake (Table 1).

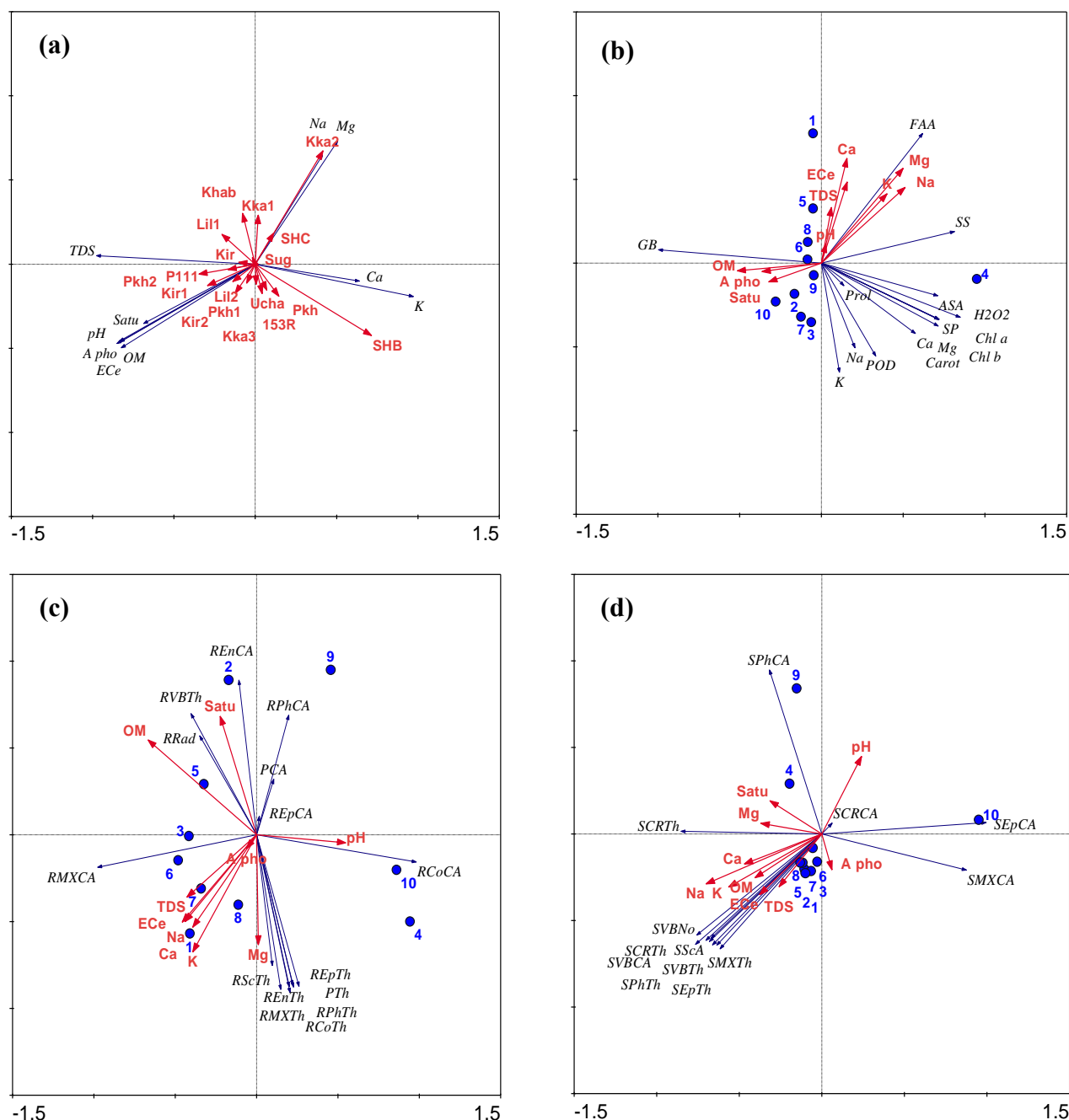


Fig. 1. RDA biplots of variation in soil characteristics among sites (a), and, CCA triplots of soil characteristics within sites plotted against on physiological attributes (b), root anatomy (c) and stem anatomy (c) of *Tamarix dioica* collected from different saline areas.

Table 1. Morphological and physiological attributes of *Tamarix dioica* collected from different habitats of Punjab, Pakistan.

	Kir	Lil1	Pkh1	Sug	Lil 2	Pkh 2	153R	P111	SHC	Khab	LSD
Morphology [Ph, Rt (cm), Sfw, Sdw (g)]											
Ph	35.0 ± 2.64a	18.6 ± 2.40de	33.3 ± 1.20ab	29.0 ± 2.08abc	15.6 ± 1.76e	24.3 ± 1.76cd	20.6 ± 2.18de	27.3 ± 0.88bc	19.4 ± 1.52de	29.5 ± 2.08abc	5.67 ^{***}
LAI	0.02 ± 0.005d	0.09 ± 0.03d	1.61 ± 0.03a	0.36 ± 0.06cd	0.30 ± 0.11cd	1.08 ± 0.39ab	0.86 ± 0.20bc	0.66 ± 0.15bcd	0.42 ± 0.15cd	0.51 ± 0.19bcd	0.58 ^{***}
Sfw	4.73 ± 0.31c	0.98 ± 0.07f	2.73 ± 0.12e	3.63 ± 0.20d	5.94 ± 0.20b	7.57 ± 0.11a	6.13 ± 0.57b	5.63 ± 0.14b	4.23 ± 0.14cd	7.93 ± 0.23a	0.75 ^{***}
Rt	17.3 ± 0.88c	8.66 ± 1.20de	28.3 ± 1.20b	15.6 ± 1.20c	5.33 ± 0.88e	53.3 ± 4.41a	13.4 ± 1.52cd	7.76 ± 0.72de	12.3 ± 1.45cd	6.33 ± 1.20e	5.25 ^{***}
Sdw	4.50 ± 0.17a	3.43 ± 0.12b	1.14 ± 0.05e	1.66 ± 0.14de	2.15 ± 0.07d	2.16 ± 0.10d	1.64 ± 0.19de	1.56 ± 0.17e	2.94 ± 0.37c	2.19 ± 0.17d	0.53 ^{***}
Lpp	15.3 ± 0.88ab	12.6 ± 1.20bcd	14.6 ± 0.88abc	12.6 ± 1.45bcd	10.3 ± 2.02cd	16.6 ± 1.45a	11.3 ± 0.88bcd	12.3 ± 1.15bcd	11.6 ± 1.20bcd	9.66 ± 1.45d	3.84 ^{***}
Photosynthetic pigments [Chl. a, b, carotenoids (mg g⁻¹fw)]											
Chl a	1.35 ± 0.004b	1.52 ± 0.003a	1.05 ± 0.003c	0.75 ± 0.002f	1.05 ± 0.005c	0.92 ± 0.003e	1.05 ± 0.003c	1.05 ± 0.002c	1.05 ± 0.004c	0.94 ± 0.003d	0.004 ^{***}
Chl b	0.45 ± 0.002a	0.41 ± 0.001b	0.33 ± 0.004g	0.39 ± 0.004c	0.31 ± 0.002i	0.36 ± 0.006e	0.34 ± 0.004f	0.32 ± 0.005h	0.36 ± 0.002e	0.37 ± 0.005d	0.005 ^{***}
Car	0.49 ± 0.003b	0.75 ± 0.006a	0.32 ± 0.001g	0.35 ± 0.002e	0.45 ± 0.004c	0.33 ± 0.002f	0.45 ± 0.005c	0.45 ± 0.003c	0.45 ± 0.005c	0.36 ± 0.002d	0.002 ^{***}
Organic osmolytes [FAA (mg g⁻¹dw); SS, SP (mg g⁻¹fw), Prol, GB (µmoles g⁻¹fw)]											
FAA	78.8 ± 2.44a	35.8 ± 3.39de	36.2 ± 3.71e	64.5 ± 2.75b	62.8 ± 2.13bc	52.3 ± 2.74c	38.3 ± 2.74d	52.6 ± 2.43c	52.0 ± 3.06c	27.7 ± 3.05e	8.49 ^{***}
SS	113 ± 6.78ab	92.7 ± 4.16b	122 ± 1.62a	123 ± 6.80a	112 ± 7.12ab	122 ± 1.72a	107 ± 1.10b	127 ± 8.60a	123 ± 2.64a	93.2 ± 3.39b	15.02 ^{***}
SP	0.02 ± 0.007c	0.09 ± 0.002bc	0.06 ± 0.001bc	0.05 ± 0.001bc	0.07 ± 0.003bc	0.13 ± 0.002b	0.01 ± 0.003c	0.31 ± 0.005a	0.02 ± 0.004c	0.04 ± 0.001bc	0.068 ^{***}
Pro	8.83 ± 2.97c	11.0 ± 3.14c	9.57 ± 2.27c	12.0 ± 3.17c	8.80 ± 2.43c	40.2 ± 2.69a	10.2 ± 2.98c	23.8 ± 4.26b	12.5 ± 1.70c	14.9 ± 1.56c	8.31 ^{***}
GB	157.2 ± 11.89	157.3 ± 9.76	164.6 ± 3.39	127.2 ± 3.57	156.8 ± 16.83	166.5 ± 6.79	161.5 ± 4.44	164.7 ± 11.40	156.3 ± 14.80	159.0 ± 11.13	39.77 ^{ns}
Oxidative stress indicators [POD (units mg⁻¹ protein), (H₂O₂ (µmol g⁻¹), ASA (µg g⁻¹fw)]											
POD	1.06 ± 0.22de	3.75 ± 0.37c	6.95 ± 0.41a	1.01 ± 0.11e	0.87 ± 0.10e	0.89 ± 0.12e	1.70 ± 0.17d	1.18 ± 0.12de	1.31 ± 0.14de	5.97 ± 0.40b	0.74 ^{***}
H ₂ O ₂	27.8 ± 4.8	28.1 ± 4.6	31.1 ± 1.2	26.8 ± 3.5	28.6 ± 4.5	29.7 ± 1.2	29.0 ± 1.6	29.0 ± 1.7	28.3 ± 1.6	26.0 ± 3.2	12.2 ^{ns}
ASA	4.87 ± 0.28a	4.15 ± 0.22abc	2.80 ± 0.13d	3.54 ± 0.28bcd	3.65 ± 0.19bcd	3.20 ± 0.13cd	3.22 ± 0.24cd	4.46 ± 0.11ab	4.33 ± 0.24ab	3.96 ± 0.28abc	0.65 ^{***}
Shoot ionic contents[mg g⁻¹dw]											
Na ⁺	47.3 ± 3.47fg	51.9 ± 3.99efg	71.0 ± 5.13bc	55.2 ± 3.47defg	57.9 ± 1.73def	65.1 ± 3.13bcd	76.9 ± 2.86ab	61.8 ± 3.99cde	83.5 ± 3.99a	44.1 ± 2.37g	11.09 ^{***}
K ⁺	20.53 ± 1.31ef	19.7 ± 0.65ef	27.2 ± 1.51ab	19.0 ± 0.65f	21.8 ± 1.29def	26.0 ± 1.08bc	24.2 ± 1.08bcd	23.0 ± 1.08cde	27.5 ± 0.65ab	29.7 ± 1.08a	3.18 ^{***}
Mg ²⁺	7.98 ± 0.15c	8.45 ± 0.22abc	8.79 ± 0.22ab	8.39 ± 0.11abc	8.48 ± 0.10abc	8.92 ± 0.28a	8.96 ± 0.23a	8.03 ± 0.12c	8.89 ± 0.10ab	8.29 ± 0.11bc	0.53 ^{***}
Ca ²⁺	8.68 ± 0.18b	8.23 ± 0.13b	9.63 ± 0.17a	6.33 ± 0.08c	6.33 ± 0.15c	8.23 ± 0.26b	8.08 ± 0.13b	8.08 ± 0.13b	8.68 ± 0.36b	8.63 ± 0.13b	0.56 ^{***}

Abbreviations are given at start of manuscript. SE values are shown. Means sharing same letters (within rows) are non-significant at $p \leq 0.05$. * = Significant at $p < 0.05$, ** = Significant at $p < 0.01$, *** = Significant at $p < 0.001$, ns = Non-significant

Organic osmolytes: Highest amino acids were found in plants collected from Kirrana hills which differed significantly from those collected from Lilla 1, Peer Khara, 153 RB and Khabbeki Lake sites. Soluble sugars were the maximum in plants inhabiting both Peer Khara sites, Sahianwala C, Katha Saghral and Pull 111. The lowest soluble sugars were recorded in plants collected from Lilla and Khabbeki Lake. Soluble proteins were the maximum in plants inhabiting Pull 111 while the lowest was recorded in populations collected from 153 RB, Kirrana hills, and Sahianwala C sites. Proline was the maximum in plants collected from Peer Khara 2 following Pull 111 sites. Glycinebetaine differed non-significantly in plants collected from all sites except those plants belonging to Katha Saghral (Table 1).

Peroxidase, hydrogen peroxide and ascorbic acid: Peroxidase was the highest in plants collected from Peer Khara and the lowest in Pull 111, Katha Saghral, Kirrana, Lilla2, Sahianwala C, 153 RB, and Peer Khara2 populations. Hydrogen peroxidase was non-significantly different in plants collected from all sites. Ascorbic acid was the highest in plants collected from Kirrana Hills and the lowest in plants inhabiting Peer Khara site (Table 1).

Root anatomical characteristics: Root epidermal thickness was the maximum in plants collected from 153 RB and the minimum in those belonging to Peer Khara 1 and Lilla 1. The endodermal cell area was the maximum in plants collected from Lilla1 and the lowest in those inhabiting Kirrana Hills, Peer Khara1 and Pull 111 sites. Vascular bundle thickness was the maximum in Lilla1 and the lowest in Sahianwala C, Katha Saghral and Peer Khara 2 populations. Pith was the thickest in plants collected from Khabbeki Lake and the thinnest in those belonging to Peer Khara1. Pith cell area was the highest in plants inhabiting Khabbeki Lake and the lowest in those collected from Peer Khara1, Katha Saghral, 153 RB and Sahianwala C sites. Root radius was the highest in plants belonging to 153 RB and the lowest in those collected from Lilla1, Peer Khara1 and 2 sites. Root metaxylem was thick in plants collected from Khabbeki Lake and the thinnest in those collected from Sahianwala C, Peer Khara1, and Katha Saghral. Metaxylem cell area was the maximum in plants inhabiting Kirrana hills and the lowest in those belonging to Sahianwala B, Katha Saghral and Khabbeki Lake sites. Phloem was the thickest in plants collected from Pull 111 and Sahianwala C site and the thinnest in 153 RB plants. Phloem cell area was the maximum in plants inhabiting Sahianwala C and Pull 111 and the lowest in 153 RB plants. Cortex was the thickest in plants collected from Katha Saghral and, intermediately thick in plants inhabiting Khabbeki, Pull 111 and Sahianwala C sites. Cortical cell area was the highest in plants collected

from Katha Saghral while plants from all other sites contained lower cell area. Epidermal cell area was the maximum in plants belonging to 153 RB and the lowest in populations collected from Lilla1, and, Peer Khara1 and 2 sites. Sclerenchyma thickness was the maximum in plants inhabiting Lilla 2 and the lowest in Khabbeki population. Endodermal thickness was the highest in plants collected from Pull 111 and lower in plants belonging to Sahianwala C, Katha Saghral, PeerKhara2, Lilla1 and 2, Khabbeki and 153 RB sites (Table 2; Fig. 2).

Stem anatomical characteristics: Stem cellular region thickness was the maximum in plants collected from Katha Saghral and the lowest in those belonging to Pull 111 and Kirrana hills. Vascular bundle thickness was the highest in plants inhabiting Lilla 2 and the lowest in those collected from Sahianwala C sites. Vascular bundle cell area was the maximum in plants inhabiting Lilla2, and the lowest in belonging to Sahianwala C. Vascular bundle number was the maximum in Lilla1 and Peer Khara1 populations and the lowest in those belonging to Katha Saghral, Sahianwala C and Khabbeki Lake sites. Metaxylem thickness was the maximum in plants inhabiting Khabbeki Lake and the lowest in plants growing at all other sites. Metaxylem cell area was the highest in plants collected from Khabbeki Lake and the lowest in those belonging to Pull 111, Katha Saghral and Sahianwala C sites. Phloem thickness was the highest in plants inhabiting Khabbeki Lake and the lowest in those belonging to Peer Khara 1 and 2, and, 153 RB sites. Phloem cell area was the maximum in plants collected from Lilla 2 and Katha Saghral sites and the lowest in those collected from Peer Khara1 and 2, and, 153 RB sites. Cortical thickness was the highest in plants inhabiting Kirrana Hills and Khabbeki Lake sites and the lowest in those collected from Katha Saghral and Pull 111 sites. The cortical cell area was the most in plants belonging to Kirrana Hills, Khabbeki Lake and 153 RB sites and lowest in those collected from all other sites. Epidermal thickness was the highest in Khabbeki Lake population and the lowest in plants from all other sites. The epidermal cell area was the maximum in plants inhabiting Khabbeki Lake. Sclerenchyma thickness was the highest in Kirrana Hills population and the lowest in plants collected from Lilla 2, Peer Khara 1 and 2, Pull 111, and Katha Saghral sites (Table 2; Fig. 3).

Canonical correspondence analysis (CCA): The CCA triplot for physiological attributes of *Tamarix dioica* is given in Figure 1. Available phosphorus, organic matter, and saturation percent were weakly influenced at 153 RB site. Free amino acids and soluble sugars were weakly influenced by sodium, potassium, calcium, and magnesium of soil at Katha Saghral. Ascorbic acid, hydrogen peroxidase, soluble proteins,

calcium, magnesium, carotenoids, peroxidase, sodium, potassium, chlorophyll *a* and chlorophyll *b* were weekly influenced by soil characters of Katha Saghral, Peer Khara, and Sahianwala C sites (Fig. 1b). The root cortical cell area strongly influenced plant height of Khabike Lake population. Root phloem cell area was influenced in plants belonging to Sahianwala C site. Root endodermal cell area was weekly influenced by soil saturation percentage of Lillah 1. Root radius and root vascular bundle thickness were weekly influenced by organic matter at Lillah 2 site. Root metaxylem cell area was linked to soil physico-chemical properties of Peer Khara 1 and 2 sites. Soil sodium, potassium, calcium, electrical conductivity, and total dissolved solids strongly influenced morpho-anatomical attributes of Kirrana Hills and 153 RB populations. Root sclerenchyma thickness, root epidermal thickness, root endodermal thickness, pith thickness, root phloem

thickness, root metaxylem thickness, and root cortical thickness were weekly influenced in plants inhabiting Pull 111 site (Fig. 1c). A higher influence of stem epidermal cell area on plant height at Khabke Lake was observed. Metaxylem cell area showed a week influence of Khabke Lake, and Peer Khara sites 1 and 2 populations. Phloem cell area was weekly influenced by soil magnesium and saturation percent of Sahianwala C and Katha Saghral. Cortical thickness was weekly linked with soil magnesium and saturation percent of Katha Saghral. Vascular bundle number, cortical thickness, sclerenchyma thickness, vascular bundle thickness and cell area, phloem thickness, metaxylem thickness, and epidermal thickness were influenced by soil sodium, potassium, calcium, electrical conductivity, total dissolved solids, and organic matter of Kirrana Hills, Likkah 1 and 2, Peer Khara 2, 153 RB and Pull 111 sites (Fig. 1).

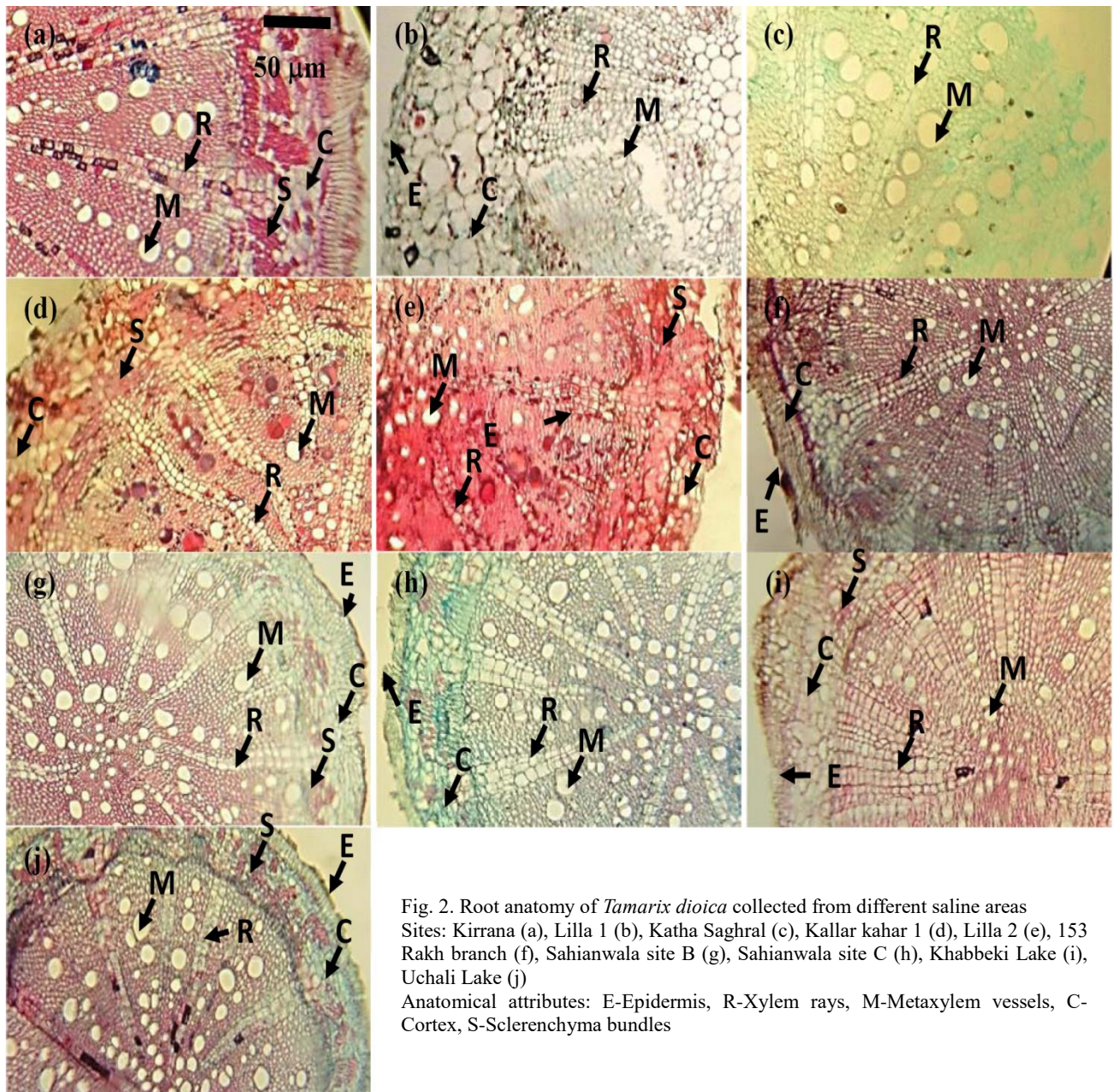


Fig. 2. Root anatomy of *Tamarix dioica* collected from different saline areas Sites: Kirrana (a), Lilla 1 (b), Katha Saghral (c), Kallar kahar 1 (d), Lilla 2 (e), 153 Rakh branch (f), Sahianwala site B (g), Sahianwala site C (h), Khabbeki Lake (i), Uchali Lake (j)
Anatomical attributes: E-Epidermis, R-Xylem rays, M-Metaxylem vessels, C-Cortex, S-Sclerenchyma bundles

Table 2. Root and stem anatomical attributes of *Tamarix dioica* collected from different habitats of Punjab, Pakistan.

	Kir	h1l	Pkh1	Sug	Lil2	Pkh2	153R	P111	SHC	Khab	LSD	
	Root Anatomy [EpiTh, VBTh, PithTh, ScTh, EndoTh, PhTh, MXTh, CortTh(□m), EndCA, PithCA, MXCA, PhCA, CortCA, EpiCA, (mm²), Radius (mm)]											
EpiTh	33.08±4.73f	80.35±2.28c	79.46±4.73c	33.08±8.19f	90.78±8.19a	47.26±6.39e	33.08±8.19f	75.62±9.75d	85.08±8.52b	77.33±4.19cd	3.33 ^{***}	
EndCA	421.2±26.1e	368.6±17.7ef	631.9±21.6d	1200.0±35.7b	368.6±28.5ef	895.2±39.5c	263.3±19.9f	2177.6±91.3a	438.6±31.6e	263.3±18.3f	78.1 ^{***}	
VBTh	170.1±6.4a	94.53±8.9cd	80.35±3.1cde	66.17±2.6e	66.17±5.2e	141.8±6.6b	94.53±8.3cd	75.62±6.6de	103.98±5.4c	103.98±2.8c	24.8 ^{***}	
PithTh	17.90±2.51	17.07±1.39	26.32±4.73	18.87±8.16	23.63±4.19	17.55±4.73	39.19±4.73	22.56±4.73	24.94±5.52	25.38±4.73	23.33 ^{ns}	
PithCA	242.8±14.6bc	210.6±12.9c	263.30±19.7bc	211.36±14.6c	304.30±12.6bc	212.92±15.7c	417.48±19.1a	347.67±10.4ab	203.87±14.7c	210.64±19.4c	110.9 ^{**}	
RR	1474±83.8c	1134±122.9e	1115.4±103.1e	600±103.1f	1677±165.6b	1370±162.6d	1616±125.2b	1677±162.3b	685±62.6e	1725±131.5a	31.67 [*]	
MXTh	119.81±14.9c	103.98±17.6d	113.44±8.9cd	80.35±14.7e	118.16±24.8c	56.72±21.8f	146.52±12.5b	167.40±9.1a	56.72±8.9f	174.88±16.9c	14.3 ^{**}	
MXCA	23246±330a	7793±147bc	7899±348bc	2633±170cd	10321±205b	2106±251de	14166±482b	29226±169a	1579±329e	25181±489a	6287 ^{**}	
PhTh	42.96±4.73a	22.04±8.19c	30.48±4.73b	23.65±4.7c	25.31±8.19c	26.34±8.19c	32.37±4.73b	26.71±5.12b	26.12±4.20c	37.57±4.73ab	7.05 ^{**}	
PhCA	1695.0±52.7a	368.6±25.7c	368.6±13.9c	263.3±15.7e	263.3±19.6e	269.3±23.9e	307.3±49.7d	263.0±13.4e	266.3±93.4e	445.9±13.9b	30.4 ^{***}	
CortTh	33.08±4.1e	64.41±12.5d	83.41±7.1fa	56.20±6.4e	66.67±7.52cd	75.62±8.19b	42.54±4.73d	72.46±8.19bc	28.36±7.48ef	23.63±3.6f	6.91 ^{***}	
CortCA	368.3±26.6i	1702±178.9d	4591.6±190.1a	1053.3±21.0f	1474.7±62.1e	1948.5±27.8c	631.9±21.6g	2001.3±169.7b	473.9±38.4h	263.5±4.2j	20.12 ^{ns}	
EPICA	368.6±15.9e	2827.5±52.6	2264.4±52.2bc	368.6±39.4e	5026.9±98.9a	1053.2±91.6de	634.8±25.7e	1369.2±273.9cd	1658.8±172.3c	1355.7±34.5cd	723.03 [*]	
ScTh	170.3±20.6b	Absent	Absent	47.6±12.5f	56.7±33.2e	158.7±20.6c	Absent	Absent	94.5±20.6d	226.8±18.1a	6.4 ^{***}	
EndoTh	37.81±12.5	23.63±1.72	56.72±8.19	42.54±8.19	23.63±9.46	47.26±8.19	23.63±4.73	89.80±8.19	42.54±6.58	23.63±8.19	23.77 ^{ns}	
	Stem Anatomy [CellRTh, VBTh, MXTh, PhTh, CRTh, EpiTh (µm), EpiCA, VBCA, SeA, CRCA, PhCA, MXCA (mm²) VBNo]											
CellRTh	1072.9±25.4e	1602.3±180.8d	1677.9±125.2d	2457.8±165.6a	1890.6±84.8cd	2046.6±98.4bcd	1692.1±45.1d	1195.8±25.5e	2056.1±87.8bc	2316.0±85.3ab	37.9 ^{***}	
VBTh	335.9±21.4dd	449.3±25.4bb	373.4±20.6d	326.1±16.3d	732.6±19.8a	259.9±18.8e	363.5±5.4e	411.2±9.5c	226.8±21.8f	501.2±36.6b	9.76 ^{***}	
VBCA	56137±1314h	127546±1458b	90946±1254d	64721±8454df	261989±1925a	39917±2333i	60350±1051g	106482±5212c	22802±725j	80256±918e	373.9 ^{***}	
VBNo.	1087.1±25.4	1654.3±25.7	1607.0±87.8	756.26±25.2	1370.7±25.4	1181.6±24.4	1039.8±87.8	1323.4±26.2	661.73±17.6	756.26±86.2	681.3 ^{ns}	
MXTh	127.6±16.3	80.5±12.5	85.8±21.6	61.4±12.5	89.8±20.2	94.5±25.6	75.6±12.5	56.7±8.9	66.1±9.4	779.2±10.8	110.5 ^{ns}	
MXCA	8373.2±238a	4212.9±574d	4528.9±236d	2001.1±130f	5529.4±362c	6266.7±564b	2949.0±319e	1790.5±291fg	1263.8±165g	3406.1±854e	515.1 ^{**}	
PhTh	122.9±20.6e	127.8±12.2e	99.6±16.9f	255.4±24.5b	193.9±25.4bd	99.6±16.9f	80.5±20.2g	245.7±21.5c	189.6±17.6d	456.2±57.2a	7.55 ^{***}	
PhCA	8531.2±166f	8899.8±162f	5687.4±242g	25334.±356a	23697.7±279b	4370.9±158h	3370.3±174i	9900.4±348e	18642.1±446c	11312±421d	956.8 ^{***}	
CRTh	217.4±28.7a	132.3±17.6c	75.6±20.2fg	70.9±8.9g	108.7±12.5d	85.8±16.9e	146.5±12.2b	70.9±8.9g	80.5±12.2ef	217.4±28.8a	5.39 ^{**}	
CRCA	16106.2±962	7425.3±486	4318.2±355	3054.8±405	4265.6±525	2949.0±726	7741.2±943	2422.4±691	4212.9±574	16241.5±878	6648 ^{ns}	
EpiTh	70.9±16.39	70.9±16.9	103.9±12.5	70.9±8.9	94.5±20.6	70.9±16.9	103.8±9.4	80.5±12.5	85.8±8.9	510.4±24.5	46.03 ^{ns}	
EpiCA	2949.±135	3212±324	5266.1±697	1263.8±182	6530.0±370	3054.3±462	1527.1±369	1474.5±380	2264.4±535	84680±744	6794 ^{ns}	
SeA	439.3±70.2a	412.2±93.8b	193.7±20.6g	207.9±20.6f	165.43±25.4h	193.7±17.6g	302.5±33.1bd	160.7±10.6h	245.7±20.6e	349.7±28.7c	12.61 ^{**}	

Abbreviations are given at start of manuscript. SE values are shown. Means sharing same letters (within rows) are non-significant at $p \leq 0.05$. * = Significant at $p < 0.05$, ** = Significant at $p < 0.01$, *** = Significant at $p < 0.001$, ns = non-significant

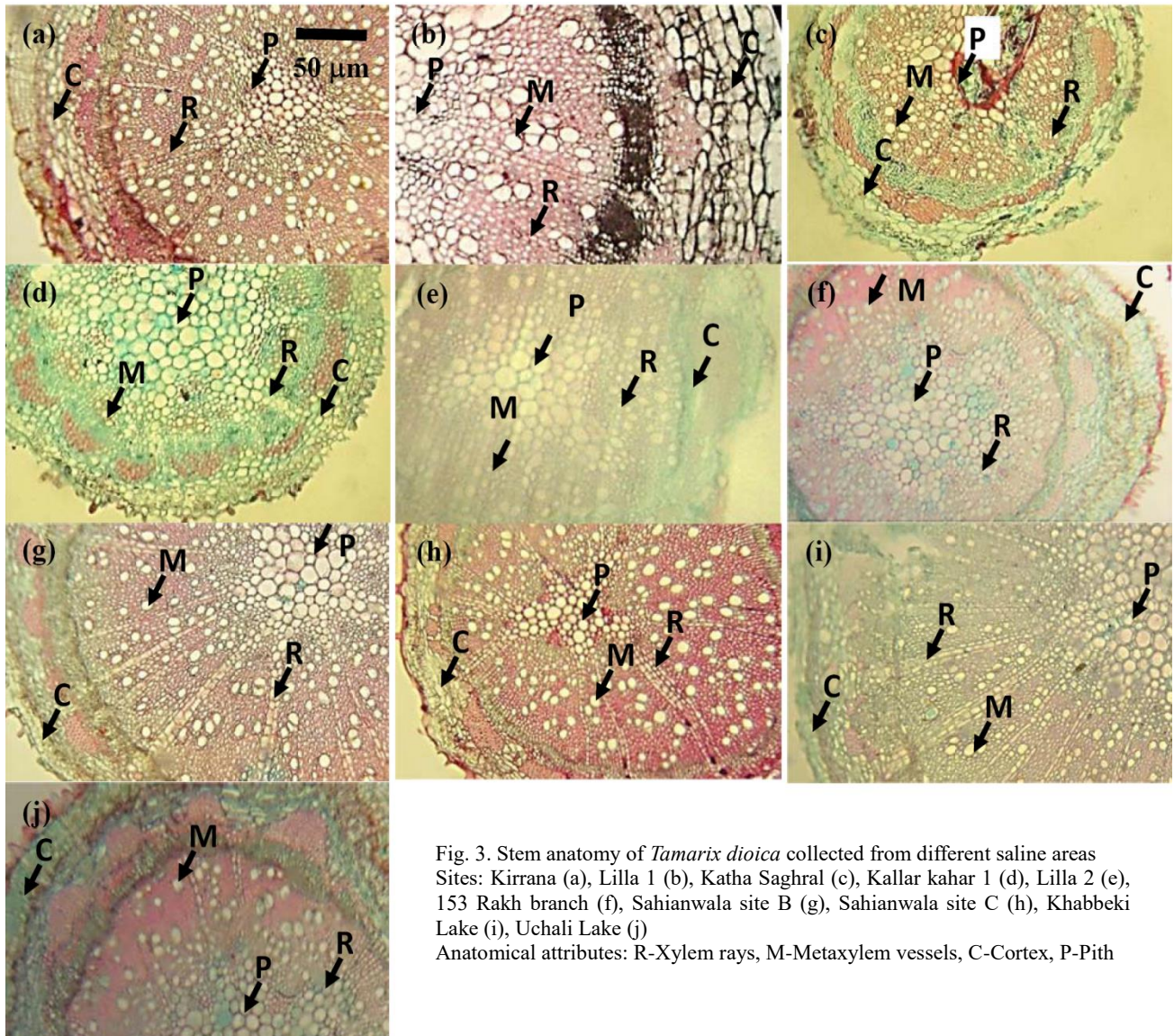


Fig. 3. Stem anatomy of *Tamarix dioica* collected from different saline areas Sites: Kirrana (a), Lilla 1 (b), Katha Saghral (c), Kallar kahar 1 (d), Lilla 2 (e), 153 Rakh branch (f), Sahianwala site B (g), Sahianwala site C (h), Khabbeki Lake (i), Uchali Lake (j)
Anatomical attributes: R-Xylem rays, M-Metaxylem vessels, C-Cortex, P-Pith

Discussion

The ecotypes of *Tamarix dioica* collected from hypersaline areas behaved differently to salinity levels of their native habitats. In populations from highly saline areas, potassium and calcium accumulated to a much higher degree which help cope with the salinity successfully by neutralizing the toxic effects of sodium concentration (Gonzalez *et al.*, 2000; Netondo *et al.*, 2004). Chlorophyll *a*, chlorophyll *b* was higher in plants belonging to hypersaline environments, while in other plants, chlorophyll contents decreased (Xia *et al.*, 2017). Magnesium was also high, which helps maintain metabolic processes and repair the membrane damage during salinity stress (Abugoch *et al.*, 2009; Xia *et al.*, 2021). Enzymatic antioxidants like peroxidase and non-enzymatic antioxidants like ascorbic acid in higher concentrations sequester reactive oxygen species (Arora *et al.*, 2012). Glycinebetaine and proline were high, indicating their crucial role as osmoprotectant under salinity stress. Soluble sugars and soluble proteins accumulated in high quantities in populations growing in heavily salt-affected soils (Mahmood & Athar, 2003). The elevated levels of glycine betaine under salinity stress are regarded as a defensive

strategy due to its role in osmoregulation and membrane stability (Flowers & Colmer, 2008).

Root epidermal thickness increased, and epidermal cell area decreased intolerant populations of *T. dioica*, indicating it to be a primary mechanism against salinity because the root epidermis directly faces soil salinity (Bray & Reid, 2002). Cortical thickness and cortical cell area increased, enhancing salinity tolerance by storing extra water and toxic ions (Hameed *et al.*, 2009). In addition, the sclerenchyma thickness increased, which is a necessary adaptation under salinity stress to counter the effects of harsh conditions by providing rigidity in plant cells (Reinoso *et al.*, 2004). Increased root radius in some populations enhanced root succulence to absorb and store extra water (YuJing *et al.*, 2000). Metaxylem thickness, metaxylem cell area, phloem thickness, and phloem cell area increased to confer salinity tolerance by better water transport water through large metaxylem and photosynthate translocation through the phloem (Long *et al.*, 2021). An increase in endodermis thickness and endodermal cell area was an important factor in coping with salinity stress as it facilitates radial movement of water and ions from endodermis (Vasellati *et al.*, 2001). Pith thickness also increased, but pith cell area decreased

as it is a critical adaptation in many dicots against salinity tolerance by storing extra water (Bernstein & Kafkafi, 2002; Mansoor, 2015; Bencherif *et al.*, 2020).

For a plant to be tolerant against harsh saline environments, every tissue must play its specific role efficiently. Stem cellular region thickness increased to tolerate against the saline habitat. Cellular region thickness increased, accompanied by increased epidermis thickness, cortical thickness, vascular bundle thickness, phloem thickness, sclerenchyma thickness, and metaxylem thickness (Kheloufi & Mansouri, 2019). Vascular bundle thickness, vascular bundle number, and vascular bundle area increased to help better conduction of water than less tolerant populations (Naz *et al.*, 2013). Furthermore, an increase in the phloem thickness, the phloem cell area is an essential strategy to cope with the salinity stress and to help improve photosynthetic translocation. The increase in metaxylem thickness and cell area play an essential function against salinity stress as a significant metaxylem function provides a large amount of water in a saline habitat. Sclerenchyma thickness is an essential factor to help save water as well as provide rigidity to the plant organs (Corrêa-Ferreira *et al.*, 2019).

Conclusion

All ecotypes of *Tamarix dioica* collected from hypersaline areas behaved differently to salinity levels based on native habitats. The populations from highly saline habitats accumulated more magnesium, potassium, and calcium in shoots resulting in higher chlorophyll *a*, chlorophyll *b* contents. Antioxidants (ascorbic acid and peroxidase) and osmoprotectants (glycinebetaine, proline, soluble sugars, and soluble proteins) were higher in tolerant populations that efficiently sequestered reactive oxygen species and enhanced osmolyte based protection against salinity stress. The epidermal thickness increased, and the epidermal cell area decreased. An increase in endodermis thickness and endodermal cell area has been identified as an essential factor in coping with salinity stress's adverse effects. Cortical thickness and cortical cell area, sclerenchyma thickness, metaxylem thickness, cell area, phloem thickness, and cell area also increased, contributing to salinity tolerance linked to better water transport photosynthate translocation through the vascular bundle. All these adaptations enabled the *T. dioica* populations to adapt to saline environments of corresponding habitats differently.

Acknowledgments

This manuscript has been extracted from PhD thesis of the first author.

References

- Abugoch, L., E. Castro, C. Tapia, M. C. Añón, P. Gajardo and A. Villarroel. 2009. Stability of quinoa flour proteins (*Chenopodium quinoa* Willd.) during storage. *Int. J. food Sci. Tec.*, 44: 2013-2020.
- Amini, S., H. Ghadiri, C. Chen and P. Marschner. 2016. Salt affected soils, reclamation, carbon dynamics, and biochar: A review. *J. Soils Sed.*, 16: 939-953.
- Anonymous. 2015. Extent of salt-affected soils. <http://www.fao.org/soils-portal/soilmanagement/management-of-some-problem-soils/salt-affected-soils/more-information-on-salt-affected-soils/en/>. Anonymous. 2017. FAO Agristat. <http://www.fao.org>.
- Arora, N.K., S. Tewari, S. Singh, N. Lal and D.K. Maheshwari. 2012. PGPR for protection of plant health under saline conditions. In: *Bacteria in Agrobiolology: Stress Management*. Springer, Berlin, Heidelberg. pp. 239-258.
- Bates, L.S., R.P. Waldren and I.D. Teare. 1973. Rapid determination of proline for water stress studies. *Plant Soil*, 39: 205-207.
- Bencherif, K., F. Trodi, M. Hamidi, Y. Dalpè and A.L. Hadj-Sahraoui. 2020. Biological overview and adaptability strategies of *Tamarix* plants, *T. articulata* and *T. gallica* to abiotic stress. In: *Plant Stress Biology*. pp. 401-433. Springer, Singapore.
- Bernstein, N. and U. Kafkafi. 2002. Root growth under salinity stress. In: *Plant Roots the Hidden H*. The Hebrew Univ. of Jerusalem Rehovot and Tel Aviv Univ. Israel, p. 787-805.
- Bray, S. and D.M. Reid. 2002. The effect of salinity and CO₂ enrichment on the growth and anatomy of the second trifoliate leaf of *Phaseolus vulgaris*. *Can. J. Bot.*, 80: 349-359.
- Chaves, M., J. Flexas and C. Pinheiro. 2009. Photosynthesis under drought and salt stress: Regulation mechanisms from whole plant to cell. *Ann. Bot.*, 103: 551-560.
- Corrêa-Ferreira, M.L., E.B. Viudes, P. M.de Magalhães, A. P.de Santana Filho, G.L. Sassaki, A.C. Pacheco and C.L. de Oliveira Petkowicz. 2019. Changes in the composition and structure of cell wall polysaccharides from *Artemisia annua* in response to salt stress. *Carb. Res.*, 483: 107753.
- Daoyuan, Z., P. Borong and Y. Linke. 2003. The photogeographical studies of *Tamarix* (Tamaricaceae). *Acta Bot. Yunnanica*, 25(4): 415-427.
- Flowers, T.J. and T.D. Colmer. 2008. Salinity tolerance in halophytes. *New Phytol.*, 179: 945-963.
- Flowers, T.J., R. Munns and T.D. Colmer. 2015. Sodium chloride toxicity and the cellular basis of salt tolerance in halophytes. *Ann. Bot.*, 115: 419-431.
- Gaskin, J.F. and B.A. Schaal. 2002. Hybrid *Tamarix* widespread in US invasion and undetected in native Asian range. *Proc. Natl. Acad. Sci.*, 99(17): 11256-11259.
- Glenn, E.P., T. Anday, R. Chaturvedi, R. Martinez-Garcia, S. Pearlstein, D. Soliz, S.G. Nelson and R.S. Felger. 2013. Three halophytes for saline-water agriculture: An oilseed, a forage and a grain crop. *Environ. Exp. Bot.*, 92: 110-121.
- Goliber, T.E. 1989. Gravitational stress and lignification in aerial vs. submerged shoots of *Hippuris vulgaris*. *Physiol. Plant.*, 75: 355-361.
- Gonzalez, M.V., M. Lopez, A.E. Valdes and R.J. Ordas. 2000. Micro propagation of three berry fruit species using nodal segments from field-grown plants. *Ann. Appl. Biol.*, 137: 73-78.
- Grieve, C.M. and S.R. Grattan. 1983. Rapid assay for determination of water soluble quaternary ammonium compounds. *Plant Soil*, 70: 303-307.
- Guo, H., S. Li, J. Ye, W. Min and Z. Hou. 2021. Ionic and antioxidant system responses to Na₂SO₄ stress of two cotton cultivars differing in salt tolerance. *Pak. J. Bot.*, 53: 11-21.
- Hameed, M., M. Ashraf and N. Naz. 2009. Anatomical adaptations to salinity in cogon grass [*Imperata cylindrica* (L.) Raeuschel] from the Salt Range, Pakistan. *Plant Soil*, 322: 229-238.
- Hamilton, P.B. and D.D. Van Slyke. 1943. Amino acid determination with ninhydrin. *J. Biol. Chem.*, 150: 231-233.
- Himabindu, Y., T. Chakradhar, M.C. Reddy, A. Kanygin, K.E. Redding and T. Chandrasekhar. 2016. Salt-tolerant genes from halophytes are potential key players of salt tolerance in glycophytes. *Environ. Exp. Bot.*, 124: 39-63.

- Jasiem, T.M., N.M. Nasser and H.K. AL-Bazaz. 2019. *Tamarix aphylla* L.: A review. *Res. J. Pharm. Technol.*, 12(7): 3219-3222.
- Joshi, R., V.R. Mangu, R. Bedre, L. Sanchez, W. Pilcher, H. Zandkarimi and N. Baisakh. 2015. Salt adaptation mechanisms of halophytes: improvement of salt tolerance in crop plants. In: *Elucidation of Abiotic Stress Signaling in Plants*, Springer, New York, NY. 243-279.
- Kheloufi, A. and L.M. Mansouri. 2019. Anatomical changes induced by salinity stress in root and stem of two *Acacia* species (*A. karroo* and *A. saligna*). *Poljoprivreda I Sumarstvo*, 65(4): 137-150.
- Kumari R, P. Kumar, D. Meghawal, V. Sharma and H. Kumar. 2019. Salt-tolerance mechanisms in plants. In: *Recent Trends in Tropical Plant Research*, AkiNik Publications, New Delhi.
- Liang, L., W. Liu, Y. Sun, X. Huo, S. Li and Q. Zhou. 2017. Phytoremediation of heavy metal contaminated saline soils using halophytes: Current progress and future perspectives. *Environ. Rev.*, 25: 269-281.
- Long, R.W., C.M. D'Antonio, T.L. Dudley and K.R. Hultine. 2021. Variation in salinity tolerance and water use strategies in an introduced woody halophyte (*Tamarix* spp.). *J. Ecol.*, DOI: 10.1111/1365-2745.13758.
- Lowry, L.H., N.J. Rosebrough, A. L. Farr and R.J. Randall. 1951. Protein measurement with the folin phenol reagent. *J. Biol. Chem.*, 193: 265-275.
- Mahmood, S. and H.R. Athar. 2003. Germination and growth of *Panicum turgidum* provenance under saline conditions. *Pak. J. Biol. Sci.*, 6: 164-166.
- Mansoor, U., M. Naseer, M. Hameed, A. Riaz, M. Ashraf, A. Younis and F. Ahmad. 2015. Root morpho-anatomical adaptations for drought tolerance in *Cenchrus ciliaris* L. ecotypes from the Cholistan desert. *Phyton.*, 55: 159-179.
- Meena, M.D., R.K. Yadav, B. Narjary, G. Yadav, H. Jat, P. Sheoran, M.K. Meena, R. Antil, B. Meena and H. Singh. 2019. Municipal solid waste (MSW): Strategies to improve salt affected soil sustainability: A review. *Waste Manag.*, 84: 38-53.
- Moodie, C.D., N.W. Smith and R.A. Mc-Greery. 1959. Manual for soil fertility development in corn (*Zea mays* L.) and subsequent grain yield. *Crop Sci.*, 11: 368-372.
- Mukherjee, S.P. and M.A. Choudhuri. 1983. Implications of water stress-induced changes in the levels of endogenous ascorbic acid and hydrogen peroxide in *Vigna* seedlings. *Physiol. Plant.*, 58(2): 166-170.
- Naz, N., M. Hameed, T. Nawaz, R. Batoool, M. Ashraf, F. Ahmad and T. Ruby. 2013. Structural adaptations in the desert halophyte *Aeluropus lagopoides* (Linn.) Trin. ex Thw. under high salinity. *J. Biol. Res.*, 19: 150.
- Netondo, G.W., J.C. Onyango and E. Beck. 2004. Sorghum and salinity I. Response of growth, water relations, and ion accumulation to NaCl salinity. *Crop Sci.*, 44(3): 797-805.
- Rabhi, M., A. Castagna, D. Remorini, C. Scattino, A. Smaoui, A. Ranieri and C. Abdely. 2012. Photosynthetic responses to salinity in two obligate halophytes: *Sesuvium portulacastrum* and *Tecticornia indica*. *S. Afr. J. Bot.*, 79: 39-47.
- Reinoso, H., L. Sosa and L. Ramirez. 2004. Salt-induced changes in the vegetative anatomy of *Prosopis strombulifera* (Leguminosae). *Can. J. Bot.*, 82: 618-628.
- Rozentsvet, O., E. Bogdanova, L. Ivanova, L. Ivanov, G. Tabalenkova, I. Zakhoshyi and V. Nesterov. 2016. Structural and functional organization of the photosynthetic apparatus in halophytes with different strategies of salt tolerance. *Photosynthetica*, 54: 405-413.
- Steel, R.G.D., J.H. Torrie and D.A. Dickey. 1997. Principles and procedures of statistics: A biometrical approach. 3rd Edition, McGraw-Hill, NY.
- Vasellati, V, M. Oesterheld and D. Medan. 2001. Effects of flooding and drought on the anatomy of *Paspalum dilatatum*. *Ann. Bot.*, 88: 355-360.
- Velikova, V., I. Yordanov and A. Edreva. 2000. Oxidative stress and some antioxidant system in acid rain treated bean plants: protective role of exogenous polyamines. *Plant Sci.*, 151: 59-6.
- Wolf, B. 1982. A comprehensive system of leaf analyses and its use for diagnosing crop nutrient status. *Comm. Soil Sci. Plant Anal.*, 13(12): 1035-1059.
- Xia, J., X. Zhao, J. Ren, Y. Lang, F. Qu and H. Xu. 2017. Photosynthetic and water physiological characteristics of *Tamarix chinensis* under different groundwater salinity conditions. *Environ. Exp. Bot.*, 138: 173-183.
- Xia, J., Y. Lang, Q. Zhao, P. Liu and L. Su. 2021. Photosynthetic characteristics of *Tamarix chinensis* under different groundwater depths in freshwater habitats. *Sci. Total Environ.*, 761: 143221.
- Yemm, E.W. and A.J. Willis. 1954. The estimation of carbohydrates in plant extracts by anthrone. *Biochem. J.*, 57: 508-514.
- YuJing, Z., Z. Yong, H. ZiZhi and Y. ShunGuo. 2000. Studies on microscopic structure of *Puccinellia tenuiflora* stem under salinity stress. *Grassl. China*, 5: 6-9.

(Received for publication 28 March 2021)